

Spatial analysis of Brazil's COVID-19 response capacity: a proposal for a Healthcare Infrastructure Index

Évilly Carine Dias Bezerra (<https://orcid.org/0000-0002-9876-6260>)¹
Priscila Soares dos Santos (<https://orcid.org/0000-0002-7313-3651>)¹
Fernanda Cigainski Lisbinski (<https://orcid.org/0000-0001-9131-5996>)¹
Lázaro Cezar Dias (<https://orcid.org/0000-0003-1051-6054>)¹

Abstract *One of the concerns linked to the COVID-19 pandemic is the capacity of health systems to respond to the demand for care for people with the disease. The objective of this study was to create a COVID-19 response Healthcare Infrastructure Index (HII), calculate the index for each state in Brazil, and determine its spatial distribution within and across regions. The HII was constructed using principal component factor analysis. The adequacy of the statistical model was tested using the Kaiser-Meyer-Olkin test and Bartlett's test of sphericity. The spatial distribution of the HII was analyzed using exploratory spatial data analysis. The data were obtained from DATASUS, the Federal Nursing Council, Ministry of Health, Government Procurement Portal, and the Transparency Portal. The nine states in the country's North and Northeast regions showed the lowest indices, while the five states from the Southeast and South regions showed the highest indices. Low-low clusters were observed in Amazonas and Pará and high-high clusters were found in Minas Gerais, Rio de Janeiro, São Paulo, and Paraná.*

Key words *COVID-19, Health system infrastructure, Brazil*

¹ Programa de Pós-Graduação em Economia e Desenvolvimento, Universidade Federal de Santa Maria. Av. Roraima 1000, Cidade Universitária. 97105-900 Santa Maria RS Brasil. evillycarine@hotmail.com

Introduction

Coronaviruses are a group of easily transmitted viruses common to humans, other mammals and birds that cause respiratory, hepatic, enteric, and neurological diseases. Six species of coronavirus are known to cause illness in humans, four of which – 229E, OC43, NL63, and HKU1 – are prevalent and normally cause cold symptoms. The other two – the severe acute respiratory syndrome coronavirus (SARS-CoV) and Middle East respiratory syndrome coronavirus (MERS-CoV)¹ – are of animal origin and associated with often fatal diseases. SARS is rapidly progressive infectious disease².

In December 2019, various health facilities in China reported a number of patients with pneumonia of unknown cause. This outbreak was associated with exposures in a seafood market in Wuhan, in the Hubei province of China. On December 31, 2019, the Chinese Center for Disease Control and Prevention sent a team to monitor and investigate the epidemiological and etiological origin of this disease in conjunction with the Chinese health authorities in Wuhan and the Hubei province. The Chinese authorities identified a new type of coronavirus in the early stages of an outbreak whose main symptoms were fever and a cough with respiratory distress^{1,3}.

On January 30, 2020, the World Health Organization (WHO) declared a Public Health Emergency of International Concern due to the rapid rise in the number of cases and deaths in China caused by the new coronavirus 2019 (COVID-19). Thereafter, the WHO recommended a number of health measures, including horizontal isolation in affected regions, temperature checks at airports and subways, and the use of surveillance cameras to help map the path of contamination. However, the virus continued to spread and, on March 11, 2020, the WHO declared the outbreak to be a global pandemic⁴.

By July 3, 2020, 10,710,005 global cases of COVID-19 and 517,877 deaths had been recorded. Forty days later, on August 12, these numbers had risen by 48% and 31%, respectively, to 20,624,316 cases and 749,421 deaths. The first case in Brazil was recorded on 26 February 2020 in São Paul and the first death was notified on March 17 in the same state⁴. By July 3, 2020, Brazil had recorded 1,539,081 cases and 63,174 deaths. By August 12, these numbers had risen by 52% and 40%, respectively, to 3,180,758 cases and 104,528 deaths^{5,6}, making Brazil the coun-

try with the world's second-highest COVID-19 death toll and number of cases.

Several countries, including Brazil, have made efforts to expand the capacity of their health systems to provide the care needed for patients with respiratory complications arising from COVID-19. According to Brazil's national health information system, DATASUS⁷, Brazil has 6,237 hospitals, 5,298 of which are general hospitals and 939 specialized hospitals. The country has 446,503 hospital beds, 314,725 (70.49%) of which are SUS beds (SUS is the acronym in Portuguese for Brazil's public health service, the *Sistema Único de Saúde*) and 131,778 (29.51%) private. The majority of beds are concentrated in the Southeast Region (40.57%), followed by the Northeast (27.12%), South (16.54%), Center-West (8.5%), and North (7.27%). However, Silva⁸ points out that Brazil's hospital system is far from being able to guarantee broad-ranging quality care to the population due to a range of structural deficiencies, including the shortage of beds, medicines, and physical facilities and inadequate staffing levels and poor working terms and conditions.

The assessment of available resources and health system capacity in a given region or country is vital for the response to COVID-19, providing a valuable tool for policymakers making decisions on the allocation of public spending on the control of the spread of the coronavirus and treatment of infected persons.

This study therefore sought to create a COVID-19 response Healthcare Infrastructure Index (HII), calculate the index for each state and determine its spatial distribution within and across regions.

Methodology

This section is divided into three parts. In the first part, we present the study data and respective sources. In the second part, we provide a brief outline of the multivariate model used in the study. Finally, we explain the spatial analysis of the data.

Study data

A number of variables capable of capturing information on the following dimensions of health system capacity at state level were used to construct the COVID-19 HII: physical healthcare

structure; number of health workers; the existence of strategic COVID-19 devices; and financial resources allocated to healthcare.

The data were obtained from DATASUS⁹, the Federal Nursing Council (COFEN)¹⁰, Health Surveillance Secretariat (SVS), Government Procurement Portal¹¹, Ministry of Health¹², and Transparency Portal^{13,14}. Chart 1 shows the dimensions, variables and respective sources.

The data were standardized, which according to Fávero and Belfiore¹⁵ involves subtracting the mean and dividing by the standard deviation for each observed value of the variable.

The following subsections describe the multivariate statistical method (principal component factor analysis) used to create the index and techniques employed to analyze the spatial distribution of the HII.

Multivariate statistical model

As mentioned above, the HII was constructed using principal component factor analysis. According to Fávero and Belfiore¹⁵, this technique allows the researcher to generate uncorrelated factors through linear combinations of initial variables. According to Manly¹⁶, factor analysis makes it possible to reduce large numbers of variables into a much smaller set of factors, as follows:

$$X_p = l_{p1}F_1 + l_{p2}F_2 + \dots + l_{pj}F_j + \varepsilon_p \quad (1)$$

Where: X_p is the i th observed variable; l_p is the product of the square root of the eigenvalues of the correlation matrix multiplied by the eigenvectors of the square root of the correlations; F_j is the i th factor; and ε_p is the i th linear combination of the principal components Z_{j+1} through Z_p .

Generalized factor analysis was applied to the 21 study variables, using the factor scores to construct the HII. Based on Mingoti¹⁷, the procedures adopted can be represented as follows:

$$HII_m = \sum_{j=1}^p \left(\frac{\sigma_j^2}{\sum_{j=1}^p \sigma_j^2} F_{jm} \right) \quad (2)$$

Where: HII_m is the Healthcare Infrastructure Index of the i th state; σ^2 is the variance explained by factor j ; p is the number of selected factors; $\sum_{j=1}^p \sigma_j^2$ is the sum of the variances explained by the extracted p factors; and is the factor score of the state m for the factor j .

Before proceeding, it was necessary to measure the adequacy of the factor analysis method-

ology. For this purpose, we performed the Kaiser-Meyer-Olkin (KMO) test and Bartlett's test of sphericity. According to Fávero and Belfiore¹⁵, these tests are represented by the following two equations:

$$KMO = \frac{\sum_{l=1}^k \sum_{c=1}^k \rho_{lc}^2}{\sum_{l=1}^k \sum_{c=1}^k \rho_{lc}^2 + \sum_{l=1}^k \sum_{c=1}^k \varphi_{lc}^2} \quad (3)$$

Where: l and c are the rows and columns, respectively, of the correlation matrix; ρ are the model variables; and φ are the higher order correlation coefficients of the model variables. KMO values vary between 0 and 1, where the closer the value is to 1, the more adequate the model. According to the literature, values of more than 0.6 indicate adequacy.

According to Fávero and Belfiore¹⁵, Bartlett's test of sphericity is represented as follows:

$$X_{Bartlett}^2 = [(n-1) - \left(\frac{2k-5}{6} \right)] \ln |D| \quad (4)$$

Where: n is the sample size; k is the number of variables; and $|D|$ is the module of the determinant of the correlation matrix of the variables that make up the index. The model is adequate when the null hypothesis that the correlation matrix is an identity matrix is rejected.

Since the values frequently vary between 0 and 1, after confirming the adequacy of the method and generation of factors, the results of the index are standardized as shown by the following equation:

$$HII_m = \frac{HII_m - HII_{min}}{HII_{max} - HII_{min}} \quad (5)$$

Where: HII_{min} and HII_{max} are the minimum and maximum calculated indices, respectively. Standardization converts the maximum and minimum values to 1 and 0, respectively, where the closer the value is to 1, the better the COVID-19 response healthcare infrastructure in the respective state. To generate the factors, we used VARIMAX orthogonal rotation of factors, which, according to Hair Jr. et al.¹⁸, provides a clearer understanding of how the variables are associated and how much this characteristic positively or negatively reflects each factor.

After performing orthogonal rotation, confirming the adequacy of the statistical model and constructing the index, it was possible to assess the spatial distribution of the HII and check for the existence of clusters, using Exploratory Spatial Data Analysis (ESDA).

Chart 1. Variables and data sources, 2020.

Dimension	Variable	Access date (2020)	Description of data	Source
Physical structure	X ₁	11/06	Number of high complexity outpatient facilities*	DATASUS ⁷
	X ₂	11/06	Number of medium complexity outpatient facilities*	
	X ₃	11/06	Number of primary outpatient facilities*	
	X ₄	11/06	Number of high complexity hospitals*	
	X ₅	11/06	Number of medium complexity hospitals*	
	X ₆	11/06	Number of health centers*	
Health workers	X ₇	12/06	Number of nursing assistants	COFEN ¹⁰
	X ₈	12/06	Number of nurses	
	X ₉	11/06	Number of doctors*	DATASUS ⁷
	X ₁₀	12/06	Number of nursing technicians	COFEN ¹⁰
Strategic COVID-19 devices	X ₁₁	07/06	Number of PCR tests	Ministry of Health ¹²
	X ₁₂	07/06	Number of rapid tests	
	X ₁₃	11/06	Number of non-SUS hospital beds*	DATASUS ⁷
	X ₁₄	11/06	Number of SUS hospital beds*	
	X ₁₅	11/06	Number of ventilators*	
	X ₁₆	07/06	Number of non-SUS adult ICUs	Ministry of Health ¹²
	X ₁₇	07/06	Number of SUS adult ICUs	
Financial resources	X ₁₈	11/06	Procurement via auction, waiver and exemption from competitive bidding for COVID-19 response (R\$)	Procurement Portal ¹
	X ₁₉	10/06	Distribution of health spending (R\$)	Transparency Portal ¹³
	X ₂₀	10/06	Amount transferred directly to the state government (R\$)	Transparency Portal ¹⁴
	X ₂₁	10/06	Amount transferred directly to municipal governments(R\$)	

*Data from April 2020 obtained from the National Health Facility Register (CNES) available from DATASUS Source: Authors' elaboration.

Spatial analysis

To assess the spatial distribution of the HII across states, we used global and local Moran's I. According to Almeida¹⁹, global Moran's I measures the similarity between values at spatial locations. Positive results indicate similarity, whereby locations with high incidence of the observed variable and/or phenomenon are surrounded by locations with similarly high values, while negative values for I indicate dissimilar values, whereby high incidence locations are surrounded with locations with low values. Local Moran's I is used to assess the existence of spatial clusters of the observed phenomenon.

According to Almeida¹⁹, global Moran's I is expressed as follows:

$$I = \frac{n}{S_o} \frac{z'Wz}{z'z} \quad (6)$$

Where: n is the number of regions indexed by i and j ; z are the standardized variables; W is the spatial weights matrix; S_o is equal to $\sum_i \sum_j w_{ij}$, indicating that the inputs of the spatial weights matrix w will be added; and Wz is the mean of the standardized variables in the neighboring locations. To proceed with the spatial analysis, the result must reject the null hypothesis of spatial randomness or non-existence of clusters.

Local Moran's I was used to determine the existence of spatial clusters of IEs_m within the different states, expressed by Anselin²⁰ as follows:

$$I = \sum I_i / [S_o (\sum z_i^2 / n)] \quad (7)$$

According to Almeida¹⁹, local Moran's I (LISA) assumes that the sum of the local indicators is proportionately equal to the global Moran's I.

Results

The results of the KMO and Bartlett's tests (0.7459 and 1,715.09, respectively) confirmed the adequacy of the principal component factor analysis, meaning it was possible to proceed with the extraction of common factors. Using *varimax* rotation, which maximizes factor variance, it was possible to obtain the factors that make up the . The factor selection criterion was an eigenvalue of more than 1, resulting in the selection of three factors, as shown in Table 1.

Together, the three extracted factors explain 95.42% of the total variance of the data. The correlation coefficients for the 21 variables and their respective factors were obtained using orthogonal rotation. The factor loadings and the generated factors are shown in Table 1. The literature¹⁷ suggests a cut-off value of at least 0.50 for the selection of factor loadings.

The first factor was shown to be related to the following variables: number of high complexity outpatient facilities (x1); number of medium complexity outpatient facilities (x2); number of primary outpatient facilities (x3); number of high complexity hospitals (x4); number of medium complexity hospitals (x5); number of nursing assistants (x7); number of nurses (x8); number of doctors (x9); number of nursing technicians (x10); number of PCR tests (x11); number of rapid tests (x12); number of non-SUS hospital beds (x13); number of SUS hospital beds (x14); number of ventilators (x15); number of non-SUS adult ICUs (x16); number of SUS adult ICUs (x17); distribution of health spending (x19); and amount transferred to municipal governments (x21). Factor 1 therefore represents the physical and human resources components of general operational structure.

The second factor was related to the number of medium complexity hospitals (x5), number of health centers (x6) and amount transferred directly to the state government (x20). This factor represents initial medical care access mechanisms and the source of direct state resources. Finally, the third factor was related to number of PCR tests (x11), procurement via auction, waiver and exemption from competitive bidding for COVID-19 response (x18), and amount trans-

ferred directly to the state government (x20). The third factor was therefore related to the context of the COVID-19 pandemic, contributing to explain the functioning of hospitals in the states in response to the increased demand for healthcare.

After the formation of the factors, we proceeded to standardize the results in order to form the index, calculating the index for each state. The highest HII was found in the State of São Paulo (0.781795), followed by Minas Gerais (0.352699), both located in the Southeast Region. The lowest indices were registered in Amapá (0.045114) and Roraima (0.045722), in the county's North Region. Table 2 shows the HII_m for each state.

The indices suggest that the spatial distribution of health system infrastructure across the country is uneven, with only the State of São Paulo achieving an index higher than 0.50. Regional disparities are evident, with higher indices being concentrated in the Southeast Region and lower indices in the North Region, where there have been reports of overburdening in the health and funeral systems caused by COVID-19²¹.

To help observe the clustering of the in the states, Figure 1 shows the spatial distribution of the indices in the different locations across the country. These results were obtained using hierarchical clustering, revealing the formation of six groups constructed by performing Ward's linkage with the application of Euclidean distance. These groups were obtained using the indices presented in Table 2.

Figure 1 shows the groups where the darker the tone the higher the index, showing that states of Amapá (0.045114), Roraima (0.045722), Acre (0.045823), Rondônia (0.06500), Sergipe (0.067870), and Tocantins (0,057963) make up the lowest index group (Group 1).

Group 2 is made up of the following states: Amazonas (0.080364), Pará (0.118611), Maranhão (0.109346), Piauí (0.07648), Rio Grande do Norte (0.085771), Paraíba (0.094154), Alagoas (0.076142), Espírito Santo (0.09662), Mato Grosso (0.096832), Mato Grosso do Sul (0.082707), and the Federal District (0.11034).

Group 3 includes the states of Pernambuco (0.16726), Ceará (0.147787), Goiás (0.149312), and Santa Catarina (0.156648), while Group 4 is made up of Bahia (0.218160), Paraná (0.233039) and Rio Grande do Sul (0.229693).

The highest HII_m were found in Group 5 (Rio de Janeiro, 0.33239; and Minas Gerais, 0.352699) and Group 6 (São Paulo, 0.781795).

Although the spatial distribution of the index in the different states is dissimilar, it is necessary

Table 1. Factor loadings, communalities, variables, eigenvalues, factor variance.

Variable	Factor 1	Factor 2	Factor 3	Communality
X1	0.9427*	0.2257	0.1700	0.9685
X2	0.9563*	0.2314	0.0045	0.9681
X3	0.9207*	0.3200	-0.0147	0.9503
X4	0.9180*	0.2249	0.2988	0.9826
X5	0.8197*	0.5201*	0.0015	0.9425
X6	0.2070	0.9351*	-0.0741	0.9227
X7	0.9494*	-0.0736	0.1284	0.9232
X8	0.9546*	0.1691	0.2088	0.9835
X9	0.9783*	0.1139	0.1609	0.9960
X10	0.8392*	0.3194	0.4158	0.9791
X11	0.6132*	0.2269	0.6987*	0.9158
X12	0.9501*	0.2676	0.1341	0.9923
X13	0.9831*	0.1139	0.1187	0.9935
X14	0.9113*	0.3798	0.0961	0.9839
X15	0.9583*	0.1125	0.2551	0.9960
X16	0.9085*	0.0341	0.3953	0.9827
X17	0.9713*	0.1875	0.0403	0.9802
X18	0.0280	-0.1663	0.8877*	0.8164
X19	0.8659*	0.2166	0.3522	0.9207
X20	0.1287	0.6369*	0.6591*	0.8567
X21	0.8634*	0.4595	0.1624	0.9829
Eigenvalues	14.9575	2.5721	2.5081	-
Explained variance (%)	0.7123	0.1225	0.1194	-
Total variance (%)	0.7123	0.8347	0.9542	-

*Factor loadings of more than 0.5.

Source: Authors' elaboration.

to check for the existence of patterns of spatial dependence. For this purpose, we used global Moran's I and local Moran's I.

To detect spatial autocorrelation, we calculated univariate global Moran's I using the queen and rook contiguity criteria. Both calculations showed similar results. Based on these results, the null hypothesis of spatial randomness was rejected, thus confirming spatial autocorrelation in the HII_m data.

After confirming spatial dependence, it was possible to analyze local patterns of spatial association in the data using local Moran's I. The results showed the formation of low-low clusters in the North Region, high-high clusters in the Southeast Region, and low-high clusters in Mato Grosso do Sul, as shown in Figure 2. The statistical significance level was set at 5%.

Low-low clusters mean that the states with a low HII_m are surrounded by other states with low

HII_m . For high-high clusters, the opposite is the case, with states with better health infrastructure being surrounded by other states with similarly high levels of infrastructure. In turn, low-high clusters indicate states with low HII_m surrounded by other states with high HII_m .

Low-low clusters were found in Amazonas and Pará, while high-high clusters were observed in the South and Southeast regions (Minas Gerais, Rio de Janeiro, São Paulo, and Paraná). As mentioned above, Mato Grosso do Sul formed a low-high cluster.

Discussion

Our findings reveal that access to healthcare across Brazil is uneven and unequal, as shown by the gap between the first and last placed states (São Paulo, $HII_m = 0.781795$; and Amapá, $HII_m =$

Table 2. Health Infrastructure Index (HII_m) by state and region, 2020.

Region	State	HII_m	Region	State	HII_m
North	Rondônia	0.065007	Northeast	Sergipe	0.067870
North	Acre	0.045823	Northeast	Bahia	0.218160
North	Amazonas	0.080364	Southeast	Minas Gerais	0.352699
North	Roraima	0.045722	Southeast	Espírito Santo	0.096621
North	Pará	0.118611	Southeast	Rio de Janeiro	0.332393
North	Amapá	0.045114	Southeast	São Paulo	0.781795
North	Tocantins	0.057963	South	Paraná	0.233039
Northeast	Maranhão	0.109346	South	Santa Catarina	0.156648
Northeast	Piauí	0.076482	South	Rio Grande do Sul	0.229693
Northeast	Ceará	0.147787	Center-West	Mato Grosso do Sul	0.082707
Northeast	Rio Grande do Norte	0.085771	Center-West	Mato Grosso	0.096832
Northeast	Paraíba	0.094154	Center-West	Goiás	0.149312
Northeast	Pernambuco	0.167269	Center-West	Federal District	0.110340
Northeast	Alagoas	0.076142			

Source: Authors' elaboration based on the study data and IBGE (Brazilian Institute of Geography and Statistics)²⁷.

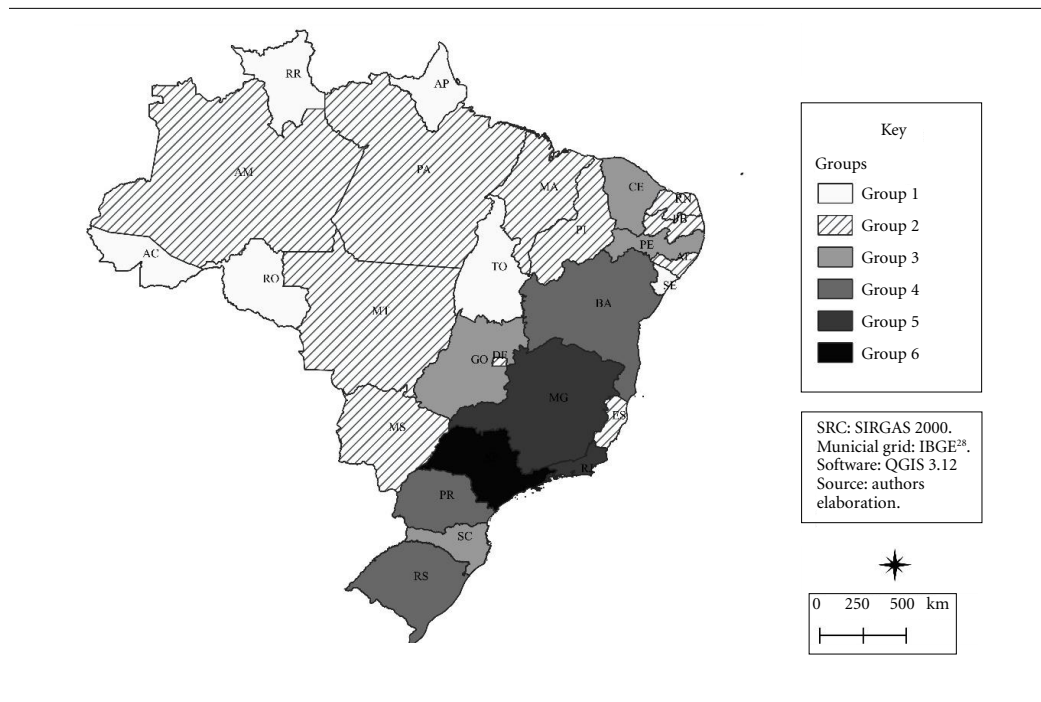


Figure 1. Spatial distribution of indices by groups.

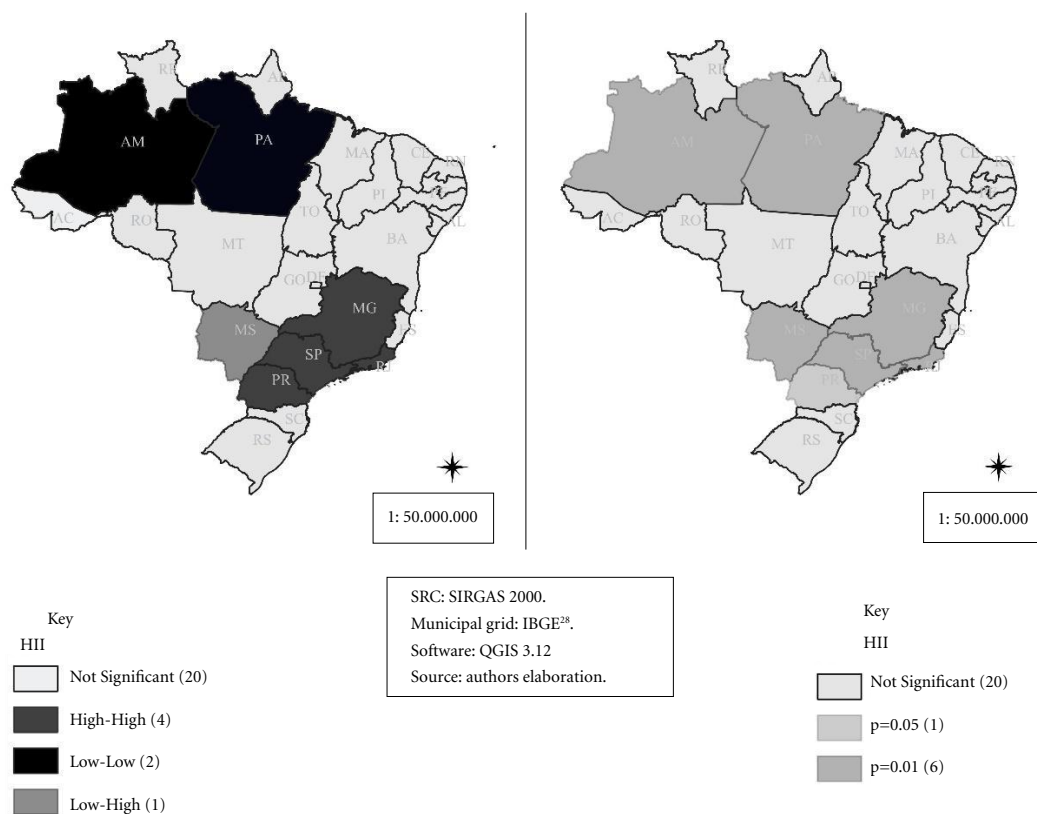


Figure 2. Clusters and significance levels achieved using ESDA.

0.045114, respectively). It is possible to note that some states are grouped with non-neighboring states from other regions. The results also show differences in health infrastructure within regions.

It is important to highlight that the states of Groups 1 and 2 – North Region and part of the Northeast and Center-West regions – have low levels of health infrastructure in comparison to the other groups. This pattern is also observed in the statistically significant spatial clusters. Specific attention should be paid to Amazonas and Pará, which form a low-low cluster, suggesting weaker health system capacity, especially in critical situations with sharp spikes in demand.

The situation of locations with a low level of health infrastructure may be aggravated by the distance between these states and those with higher , especially in the case of transfer of critically ill patients to other health facilities for example. In an analysis hospital bed availability for

the COVID-19 response in Rio Grande do Sul, Smolski et al.²² concluded that the majority of the population depends on transfers to services concentrated in regional referral centers. The authors also found inequalities in the distribution and provision of hospital beds and ventilators and some health regions lacked adult ICU beds. Pedrosa and Albuquerque²³ also investigated the distribution of COVID-19 cases and ICU beds allocated to the treatment of the disease in the State of Ceará.

Adequate infrastructure for responding to peaks in demand such as those experienced during the COVID-19 pandemic is fundamental for combating disease mortality. In this regard, Moreira²⁴ showed that health regions with the highest COVID-19 mortality rates were located in areas with a shortage of ICU beds and ventilators concentrated mainly in parts of the Northeast, Southeast, and South regions of the country.

According to Noronha et al.²⁵, the pressure

added to the health system by the demand for healthcare triggered by the COVID-19 pandemic exposes healthcare inequalities, showing that capacity is insufficient, despite the presence of the private sector. This structure should be reinforced with, for example, the creation of field hospitals combined with strategies designed to reduce the spread of the disease.

The highest HIIs were found in the Southeast Region, more specifically in São Paulo. It is important to underline that, according to the National Supplementary Health Agency (ANS)²⁶, in March 2020, the Southeast Region also accounted for the highest number of private health insurance plans, followed by the South, Northeast, Center-West, and North regions. Moreover, data from the 2008 Household Budget Survey shows that average household spending on healthcare and health insurance was highest in the Southeast Region, followed by the South, Center-West, Northeast, and North regions²⁷.

It is also important to highlight that health infrastructure alone does not necessarily reflect the vulnerability of the state to pandemics like COVID-19, as other factors like the speed at which the virus spreads, isolation indices, mask

use and other transmission reduction measures, number of inhabitants, and population density may influence the number of cases and deaths. These factors provide several directions for future research.

It is hoped that the findings of this study will contribute to public policies designed to expand health infrastructure in Brazil in order to reduce regional disparities in access to healthcare. Study limitations include the limited number of studies on COVID-19 and national trends given that the pandemic is a recent phenomenon and it is still difficult to measure its effects, thus restricting the scope of discussion of this topic. Other limitations relate to infrastructure recently implemented in response to the pandemic, making it difficult to include all relevant information in the study. In addition, it is important to bear in mind that health infrastructure is used not only for the COVID-19 response, but also for the prevention, diagnosis and treatment of other diseases. The findings should therefore be interpreted with caution, given that the health system should be prepared to tackle a range of other diseases. Future research should expand on this study using

local time series data and dynamic indices.

Collaborations

All authors participated in all stages of this study, including study conception and the drafting and revision of this manuscript.

References

1. Zhu N, Zhang D, Wang W, Li X, Yang B, Song J, Zhao X, Huang B, Shi W, Lu R, Niu P, Zhan F, Ma X, Wang D, Xu W, Wu G, Gao GF, Tan W, China Novel Coronavirus Investigating and Research Team. A novel coronavirus from patients with pneumonia in China, 2019. *N Engl J Med* 2020; 382(8):727-733.
2. Tsang KW, Ho PL, Ooi GC, Yee WK, Wang T, Chan -Yeung M, Lam WK, Seto WH, Yam LY, Cheung TM, Wong PC, Lam B, Ip MS, Chan J, Yuen KY, Lai KN. A cluster of cases of severe acute respiratory syndrome in Hong Kong. *N Engl J Med* 2003; 348(20):1975-1983.
3. World Health Organization (WHO). *Novel coronavirus: China, 2020* [Internet]. [acessado 2020 Jun 26]. Disponível em: <http://www.who.int/csr/don/12-january-2020-novel-coronavirus-china/en/>
4. Organização Pan-Americana da Saúde (OPAS). *Folha informativa - COVID-19: doença causada pelo novo coronavírus, 2020* [Internet]. [acessado 2020 Jul 04]. Disponível em: https://www.paho.org/bra/index.php?option=com_content&view=article&id=6101:-covid19&Itemid=875
5. Brasil. Ministério da Saúde (MS). *Coronavírus - COVID 19: O que você precisa saber* [Internet]. 2020 [acessado 2020 Jun 26]. Disponível em: <https://coronavirus.saude.gov.br/>
6. Brasil. Ministério da Saúde (MS). *COVID-19 no Brasil* [Internet]. 2020 [acessado 2020 Jul 4]. Disponível em: <http://susanalitico.saude.gov.br/#/dashboard/>
7. Brasil. Ministério da Saúde (MS). DATASUS. *Tabnet* [Internet]. [acessado 2020 Jun 11]. Disponível em: <https://datasus.saude.gov.br/informacoes-de-saude-tabnet/>
8. Silva HB. *Mais Médicos e o Médicos pelo Brasil, 2019* [Internet]. [acessado 2020 Jun 26]. Disponível em: http://www.portal.cfm.org.br/index.php?option=com_content&view=article&id=28381:2019-08-09-19-00-50&catid=46:artigos&Itemid=18
9. Brasil. Ministério da Saúde (MS). DATASUS. *Leitos de internação* [Internet]. [acessado 2020 Jun 26]. Disponível em: <http://tabnet.datasus.gov.br/cgi/defthtm.exe?cnes/cnv/leintbr.def>
10. Conselho Federal de Enfermagem (COFEN). *Enfermagem em números* [Internet]. [acessado 2020 Jun 12]. Disponível em: <http://www.cofen.gov.br/enfermagem-em-numeros>
11. Portal de Compras. *Painel de compras COVID-19* [Internet]. 2020 [acessado 2020 Jun 11]. Disponível em: <https://www.comprasgovernamentais.gov.br/index.php/transparencia/60-transparencia/1313-transparencia-dos-dados-de-compras-para-o-covid-19>
12. Brasil. Ministério da Saúde (MS). *Painel de leitos e insumos* [Internet]. 2020 [acessado 2020 Jun 7]. Disponível em: <https://covidinsumos.saude.gov.br/paineis/insumos/painel.php>
13. Portal da Transparência. *Saúde: Distribuição das despesas com saúde por localidade* [Internet]. 2020 [acessado 2020 Jun 10]. Disponível em: <http://www.portal-transparencia.gov.br/funcoes/10-saude?ano=2020>
14. Portal da Transparência. *Recursos transferidos* [Internet]. 2020 [acessado 2020 Jun 10]. Disponível em: <http://www.portaldatransparencia.gov.br/transferencias>
15. Fávero LP, Belfiore P. *Manual de análise de dados*. Rio de Janeiro: Elsevier; 2017.
16. Manly BFJ. *Métodos estatísticos multivariados: uma introdução*. 3ª ed. Porto Alegre: Bookman; 2008.
17. Mingoti SA. *Análise de dados através de métodos de estatística multivariada: uma abordagem aplicada*. Belo Horizonte: Editora UFMG; 2005.
18. Hair Jr JF, Black WC, Babin BJ, Anderson RE, Tatham RL. *Análise multivariada de dados*. Porto Alegre: Bookman Editora; 2009.
19. Almeida E. *Econometria espacial*. Campinas: Alínea; 2012.
20. Anselin L. Local Indicators of Spatial Association – LISA. *Geographical Analysis* 1995; 27(2):93-115.
21. Silva SG. Pandemia e afetações das emoções: reflexões sobre a realidade da Covid-19 no estado do Amapá. *Rev Bras Sociol Emoção* 2020; 19(55):113-124.
22. Smolski FMS, Battisti IDE, Soder RM, Rotta E, Kucharski KW. *Disponibilidade de leitos hospitalares e ventilação mecânica no Rio Grande do Sul: desafios no enfrentamento da COVID-19* [Internet]. 2020 [acessado 2020 Jun 25]. Disponível em: https://www.researchgate.net/publication/341651488_Disponibilidade_de_leitos_hospitalares_e_ventilacao_mecanica_no_Rio_Grande_do_Sul_desafios_no_enfrentamento_da_COVID-19
23. Pedrosa NL, Albuquerque NLS. Análise Espacial dos Casos de COVID-19 e leitos de terapia intensiva no estado do Ceará, Brasil. *Cien Saude Colet* 2020; 25(Supl. 1):2461-2468.
24. Moreira RS. COVID-19: unidades de terapia intensiva, ventiladores mecânicos e perfis latentes de mortalidade associados à letalidade no Brasil. *Cad Saude Publica* 2020; 36(5):e00080020.
25. Noronha KVMS, Guedes GR, Turra CM, Andrade MV, Botega L, Nogueira D, Calazans JÁ, Carvalho L, Servo L, Ferreira ME. Pandemia por COVID-19 no Brasil: análise da demanda e da oferta de leitos hospitalares e equipamentos de ventilação assistida segundo diferentes cenários. *Cad Saude Publica* 2020; 36(6):e00115320.
26. Agência Nacional de Saúde Suplementar (ANS). *Beneficiários* [Internet]. [acessado 2020 Jun 29]. Disponível em: http://www.ans.gov.br/anstabnet/cgi-bin/dh?dados/tabnet_br.def
27. Instituto Brasileiro de Geografia e Estatística (IBGE). *Sistema IBGE de Recuperação Automática* [Internet]. [acessado 2020 Jun 28]. Disponível em: <https://sidra.ibge.gov.br>
28. Instituto Brasileiro de Geografia e Estatística (IBGE). *Malhas municipais 2019* [Internet]. [acessado 2020 Jun 6]. Disponível em: <https://www.ibge.gov.br/geociencias/organizacao-do-territorio/15774-malhas.html?=&t=downloads>

Article submitted 16/07/2020

Approved 13/09/2020

Final version submitted 15/09/2020

